

# *Fermi*-LAT DETECTION OF GRAVITATIONAL LENS DELAYED GAMMA-RAY FLARES FROM BLAZAR B0218+357

C. C. CHEUNG<sup>1,2</sup>, S. LARSSON<sup>3,4,5,6,7</sup>, J. D. SCARGLE<sup>8,9</sup>, M. A. AMIN<sup>10</sup>, R. D. BLANDFORD<sup>11</sup>, D. BULMASH<sup>12</sup>, J. CHIANG<sup>11</sup>,  
S. CIPRINI<sup>13,14</sup>, R. H. D. CORBET<sup>15,16</sup>, E. E. FALCO<sup>17</sup>, P. J. MARSHALL<sup>18,11</sup>, D. L. WOOD<sup>19</sup>, M. AJELLO<sup>20</sup>, D. BASTIERI<sup>21,22</sup>,  
A. CHEKHTMAN<sup>23</sup>, F. D'AMMANDO<sup>24</sup>, M. GIROLETTI<sup>24</sup>, J. E. GROVE<sup>1</sup>, B. LOTT<sup>25</sup>, R. OJHA<sup>26</sup>, M. ORIENTI<sup>24</sup>,  
J. S. PERKINS<sup>26</sup>, M. RAZZANO<sup>27,28</sup>, A. W. SMITH<sup>29</sup>, D. J. THOMPSON<sup>26</sup>, K. S. WOOD<sup>1</sup>

*ApJL, accepted for publication*

## ABSTRACT

Using data from the *Fermi* Large Area Telescope (LAT), we report the first clear  $\gamma$ -ray measurement of a delay between flares from the gravitationally lensed images of a blazar. The delay was detected in B0218+357, a known double-image lensed system, during a period of enhanced  $\gamma$ -ray activity with peak fluxes consistently observed to reach  $> 20 - 50\times$  its previous average flux. An auto-correlation function analysis identified a delay in the  $\gamma$ -ray data of  $11.46 \pm 0.16$  days ( $1\sigma$ ) that is  $\sim 1$  day greater than previous radio measurements. Considering that it is beyond the capabilities of the LAT to spatially resolve the two images, we nevertheless decomposed individual sequences of superposing  $\gamma$ -ray flares/delayed emissions. In three such  $\sim 8 - 10$  day-long sequences within a  $\sim 4$ -month span, considering confusion due to overlapping flaring emission and flux measurement uncertainties, we found flux ratios consistent with  $\sim 1$ , thus systematically smaller than those from radio observations. During the first, best-defined flare, the delayed emission was detailed with a *Fermi* pointing, and we observed flux doubling timescales of  $\sim 3 - 6$  hrs implying as well extremely compact  $\gamma$ -ray emitting regions.

*Subject headings:* Galaxies: active — gravitational lensing: strong — gamma rays: galaxies — quasars: individual (B0218+357)

<sup>1</sup> Space Science Division, Naval Research Laboratory, Washington, DC 20375-5352, USA

<sup>2</sup> email: Teddy.Cheung@nrl.navy.mil

<sup>3</sup> Department of Physics, Stockholm University, AlbaNova, SE-106 91 Stockholm, Sweden

<sup>4</sup> The Oskar Klein Centre for Cosmoparticle Physics, AlbaNova, SE-106 91 Stockholm, Sweden

<sup>5</sup> Department of Astronomy, Stockholm University, SE-106 91 Stockholm, Sweden

<sup>6</sup> Supported by the Royal Swedish Academy Crafoord Foundation

<sup>7</sup> email: stefan@astro.su.se

<sup>8</sup> Space Sciences Division, NASA Ames Research Center, Moffett Field, CA 94035-1000, USA

<sup>9</sup> email: Jeffrey.D.Scargle@nasa.gov

<sup>10</sup> Kavli Institute for Cosmology and Institute of Astronomy, University of Cambridge, Madingley Road, Cambridge CB3 0HA, UK

<sup>11</sup> W. W. Hansen Experimental Physics Laboratory, Kavli Institute for Particle Astrophysics and Cosmology, Department of Physics and SLAC National Accelerator Laboratory, Stanford University, Stanford, CA 94305, USA

<sup>12</sup> Department of Physics, Stanford University, Stanford, CA 94305, USA

<sup>13</sup> Agenzia Spaziale Italiana (ASI) Science Data Center, I-00133 Roma, Italy

<sup>14</sup> Istituto Nazionale di Astrofisica - Osservatorio Astronomico di Roma, I-00040 Monte Porzio Catone (Roma), Italy

<sup>15</sup> Center for Research and Exploration in Space Science and Technology (CREST) and NASA Goddard Space Flight Center, Greenbelt, MD 20771, USA

<sup>16</sup> University of Maryland Baltimore County, Baltimore, MD 21250, USA

<sup>17</sup> Harvard-Smithsonian Center for Astrophysics, Cambridge, MA 02138, USA

<sup>18</sup> Department of Physics (Astrophysics), Oxford University, Oxford OX1 3RH, UK

<sup>19</sup> Praxis Inc., Alexandria, VA 22303, resident at Naval Research Laboratory, Washington, DC 20375, USA

<sup>20</sup> Space Sciences Laboratory, 7 Gauss Way, University of California, Berkeley, CA 94720-7450, USA

<sup>21</sup> Istituto Nazionale di Fisica Nucleare, Sezione di Padova, I-35131 Padova, Italy

<sup>22</sup> Dipartimento di Fisica e Astronomia “G. Galilei”, Università di Padova, I-35131 Padova, Italy

<sup>23</sup> Center for Earth Observing and Space Research, College of Science, George Mason University, Fairfax, VA 22030, resident at Naval Research Laboratory, Washington, DC 20375, USA

<sup>24</sup> INAF Istituto di Radioastronomia, 40129 Bologna, Italy

<sup>25</sup> Centre d'Études Nucléaires de Bordeaux Gradignan, IN2P3/CNRS, Université Bordeaux 1, BP120, F-33175 Gradignan Cedex, France

<sup>26</sup> NASA Goddard Space Flight Center, Greenbelt, MD 20771, USA

<sup>27</sup> Istituto Nazionale di Fisica Nucleare, Sezione di Pisa, I-56127 Pisa, Italy

<sup>28</sup> Funded by contract FIRB-2012-RBFR12PM1F from the Italian Ministry of Education, University and Research (MIUR)

<sup>29</sup> Department of Physics and Astronomy, University of Utah, Salt Lake City, UT 84112, USA

## 1. INTRODUCTION

B0218+357 was discovered with the NRAO 140-ft telescope in its strong source survey (S3 0218+35; Pauliny-Toth & Kellermann 1972). Later radio imaging revealed it to be a gravitationally lensed blazar with the smallest separation double-image known (335 milliarcseconds), and an Einstein ring with a similar angular diameter (O’Dea et al. 1992; Patnaik et al. 1993). The lens galaxy is at redshift  $z = 0.6847$  (Browne et al. 1993), and the blazar was later securely measured at  $z = 0.944 \pm 0.002$  (Cohen et al. 2003).

Shortly after the lens discovery, Corbett et al. (1996) measured a time delay (Refsdal 1964)  $\Delta t_r = 12 \pm 3$  days ( $1\sigma$  quoted throughout unless otherwise specified) at radio wavelengths, using the VLA to spatially separate and monitor the polarization variability in its leading brighter A (western) and fainter B (eastern) images. Later independent (but contemporaneous) dual-frequency VLA observations further refined the delay,  $\Delta t_r = 10.5 \pm 0.2$  (Biggs et al. 1999) and  $10.1 \pm 0.8$  days (Cohen et al. 2000). Interestingly, Eulaers & Magain (2011) analyzed the latter’s measurements and found two possible delays,  $\Delta t_r = 9.9^{+4.0}_{-0.9}$  or  $11.8 \pm 2.3$  days. Although these delays span a narrow range,  $\Delta t_r \sim 10 - 12$  days, because of the differing assumptions and analysis techniques employed in these works, there remains some debate on how to best derive their uncertainties.

B0218+357 is also a  $\gamma$ -ray source detected by the *Fermi* Large Area Telescope (LAT; Atwood et al. 2009) with an average flux<sup>30</sup>  $F_\gamma = (1.00 \pm 0.07) \times 10^{-7}$  photons  $\text{cm}^{-2} \text{s}^{-1}$  over its first 2-years of observations (2FGL J0221.0+3555; Nolan et al. 2012). Its steep spectrum at  $> 100$  MeV energies (photon index,  $\Gamma = 2.28 \pm 0.04$ ) and overall spectral energy distribution are typical of an otherwise normal  $\gamma$ -ray emitting flat-spectrum radio quasar (e.g., Ghisellini et al. 2010). While  $\gamma$ -ray data lack the necessary spatial resolution to separate lensed images, such blazars display their most dramatic variability in  $\gamma$ -rays, and the LAT’s all-sky monitoring could give it a distinct advantage over lower-frequency imaging observations in parameterizing lensed systems. Indeed, Atwood (2007) proposed prior to *Fermi*’s launch that the LAT could detect delayed emission from such gravitationally lensed blazars using integrated lightcurves for sufficiently bright  $\gamma$ -ray flares. B0218+357 was found to be variable in the early LAT observations, though only modestly so (Abdo et al. 2010, see Figure 1).

Bright  $\gamma$ -ray flaring from B0218+357 was detected with the LAT beginning late 2012 August (Ciprini 2012), and a delayed flare was tentatively identified  $\sim 10$  days later (Giroletti et al. 2012), consistent with the radio delay measurements. The blazar then displayed even brighter, more sustained flaring activity beginning September 14, thus prompting a *Fermi* Target-of-Opportunity (ToO) pointed observation (Cheung et al. 2012) that traced the anticipated delayed emission in detail. Two main additional flaring events were subsequently observed in as many months (see Figure 1 for an overview). We discuss the  $\gamma$ -ray temporal and spectral properties of B0218+357 together with the derived time lag, flare timescales, and observed flux ratios of the A/B

images.

## 2. LAT OBSERVATIONS AND ANALYSIS

The *Fermi*-LAT operates in a default sky-survey mode, and over every two  $\sim 1.6$ -hr spacecraft orbits, provides observations covering the entire sky. We used LAT observations with the P7SOURCE\_V6 instrument response functions, selecting 100 MeV – 100 GeV events with a region of interest (ROI) of radius =  $15^\circ$  centered at the B0218+357 radio position, R.A. =  $35^\circ.27279$ , Decl. =  $35^\circ.93715$  (J2000; Patnaik et al. 1992). The maximum zenith angle of  $100^\circ$  was set to minimize the contamination from Earth limb photons as well as the appropriate `gtmktime` filter (#3) following the FSSC recommendations<sup>31</sup> for the combination of sky-survey and pointed observations. The `gtlike` likelihood in the *Fermi* Science tools (version `v9r27p1`) was used for the spectral analysis, assuming throughout a single power-law model for B0218+357 over the selected energy range (as in the 2FGL catalog). The background model included all 2FGL sources within the ROI as well as the Galactic (`gal_2yearp7v6_v0.fits`) and isotropic (`iso_p7v6source.txt`) diffuse components.

In generating each lightcurve, the isotropic normalization was left free to vary in each time-bin while the two known variable 2FGL sources within a  $5^\circ$  ROI and the Galactic normalization were initially fitted over each full interval, then fixed at the average fitted values in the shorter time-bins. As a convenient reference point, we define  $T = \text{MJD} - 56100$  days (i.e.,  $T = 0$  was 2012 June 22), the time when  $\gamma$ -ray flaring became obvious. Integrating 1417 days ( $\sim 3.9$  years) of LAT observations prior to this date gave an average  $F_\gamma = (0.83 \pm 0.05) \times 10^{-7}$  photons  $\text{cm}^{-2} \text{s}^{-1}$ , with  $\Gamma = 2.30 \pm 0.03$ , consistent with the 2FGL value. For context, we generated a 1-week binned lightcurve for 5-years of data (2008 August 5 - 2013 August 6; Figure 1, top) assuming a fixed  $\Gamma = 2.3$ . Besides the modest source activity in early 2009 and 2010, the pronounced flaring beginning in mid-2012 lasting for  $\sim 200$  days is apparent; thereafter, the source quieted again to earlier levels.

In order to study the flaring activity in detail, we defined a 265-day interval starting at  $T = 0$  days and generated 1-day and 6-hr binned lightcurves. The *Fermi* ToO observations also allowed us to produce a  $\sim 1.6$ -hr orbit-by-orbit binned lightcurve for the sub-interval covering the first delayed flare from 2012 September 24 - October 1 ( $T = 94 - 101$  days). To search for any possible spectral changes, we initially computed the 1-day binned lightcurve with the photon index free in the fit. For the 108 points with the greatest significance (test statistic<sup>32</sup>,  $TS \geq 25$ ), we found all but four points within  $2\sigma$  of the weighted average value of  $2.31 \pm 0.02$ , which in turn is consistent with the 3.9-yr average. We thus regenerated the 1-day (Figure 1, middle), the 1.6-hr orbit (Figure 1, bottom), and the 6-hr binned lightcurves (Figure 2) with  $\Gamma = 2.3$  fixed.

## 3. RESULTS

<sup>31</sup> [http://fermi.gsfc.nasa.gov/ssc/data/analysis/documentation/Cicerone/Cicerone\\_Likelihood/Exposure.html](http://fermi.gsfc.nasa.gov/ssc/data/analysis/documentation/Cicerone/Cicerone_Likelihood/Exposure.html)

<sup>32</sup> The source significance is equivalent to  $\sim \sqrt{TS}$ , assuming one degree of freedom (Mattox et al. 1996).

<sup>30</sup> LAT  $\gamma$ -ray fluxes are reported at  $E > 100$  MeV throughout.

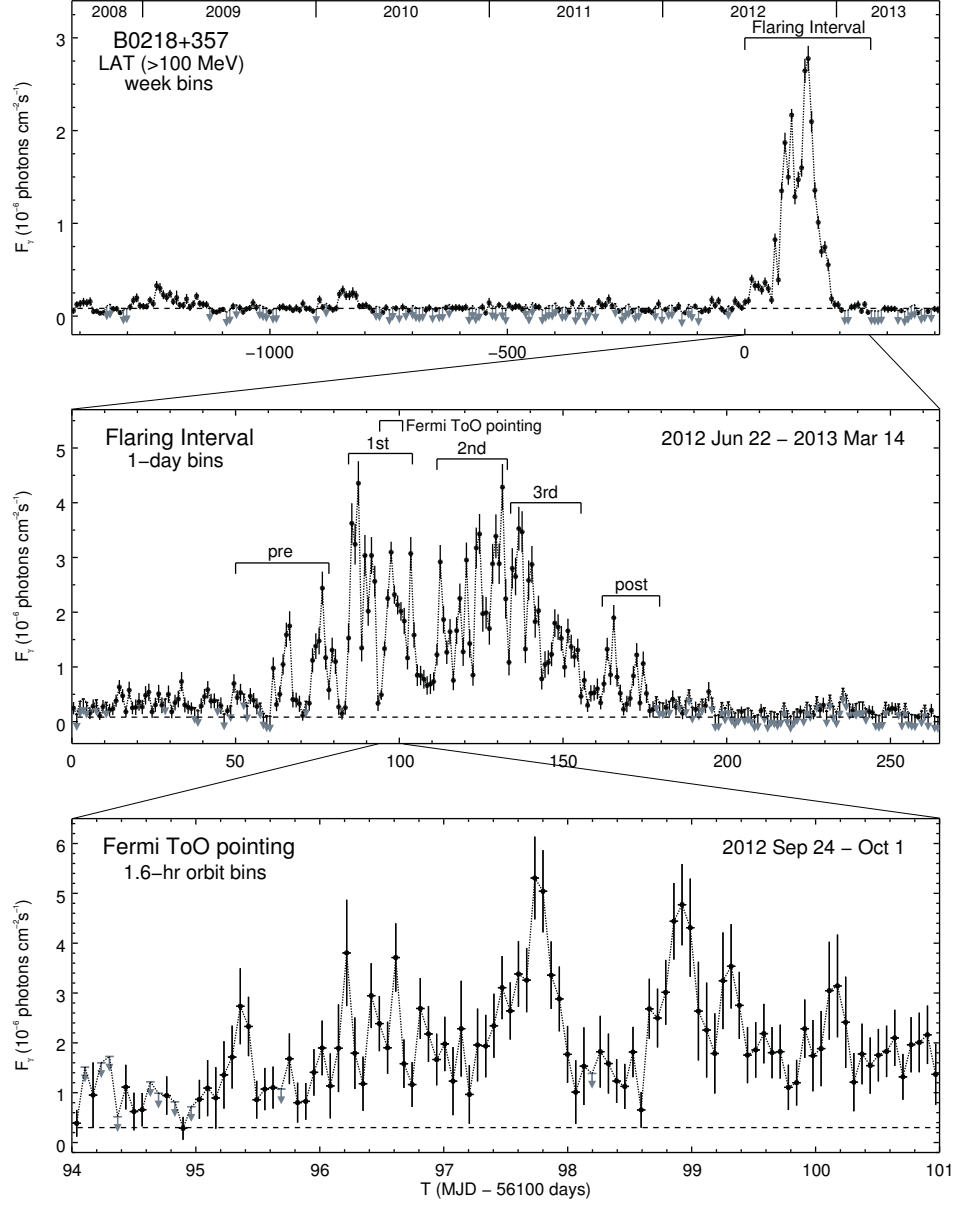


FIG. 1.— LAT lightcurves over wide dynamic range: 1-week bins over the first 5-years of the *Fermi* mission (top), 1-day bins for a 265-day flaring interval (middle), and 1.6-hr orbit bins during the 7-day *Fermi* ToO (bottom). The pre, post, and three active episodes outlined in the middle panel are further detailed in Figure 2. Throughout, flux points (plotted with  $1\sigma$  errors when  $TS \geq 4$  in the bin) and arrows indicating  $2\sigma$  upper limits (when  $TS < 4$ ) are connected by dotted lines. Horizontal dashed lines indicate the 3.9-year average flux prior to the flaring interval (top) and the baseline flux during the flaring interval,  $F_\gamma = 0.3 \times 10^{-6}$  photons  $\text{cm}^{-2} \text{s}^{-1}$  (middle, bottom).

### 3.1. Time Lag

The B0218+357  $\gamma$ -ray lightcurve appears quite complex with many peaks and valleys over the  $\sim 4$  months from  $T \sim 60 - 180$  days (Figure 2) when the source was most active. To search for a time lag, we computed the auto-correlation function (ACF) for the 6-hr binned lightcurve up to lag values of half of the total defined 265-day flaring interval. This evenly sampled lightcurve consisted of 1057 measurements with three missing data points due to exposure gaps. The ACF was therefore computed both by a standard (after interpolating the three missing points) and a discrete routine (Edelson & Krolik 1988). The two procedures gave al-

most identical results and the ACF is shown in Figure 3. A single prominent correlation peak is apparent between the time lag range of 11 – 12 days. The peak’s significance is  $9\sigma$  with respect to the measurement noise and comparing it to the height above the ACF “background.” Fitting a Gaussian function to this peak, we estimated a best-fit value,  $\Delta t_\gamma = 11.46 \pm 0.16$  days ( $1\sigma$ ). Uncertainties were estimated by a model independent Monte Carlo method (Peterson et al. 1998) accounting for the effects of measurement noise and data sampling. The time lag does not match any known period observed with the LAT (Ackermann et al. 2012; Corbet et al. 2012). Because the  $\gamma$ -ray flaring was so pronounced especially from

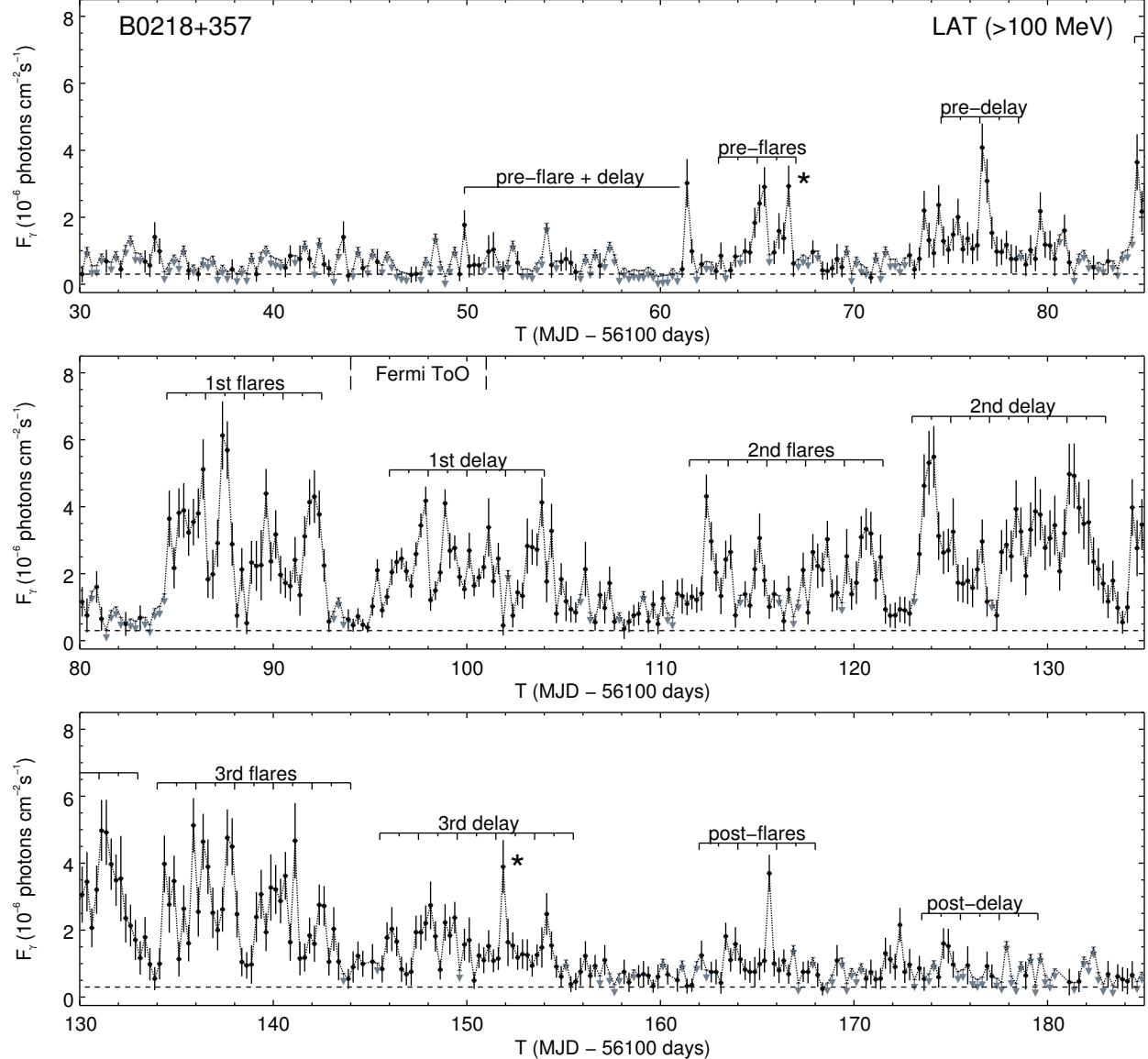


FIG. 2.— LAT lightcurve in 6-hr bins from 2012 July 22 - December 24 detailing the pre, post, and three main episodes (cf., Figure 1, middle), sub-divided into  $\sim 8 - 10$  day-long flares and corresponding delays (asterisks mark outlying sharp features; see text). Each panel spans 55-days, with adjacent panels overlapping by 5-days on each side. Horizontal dashed lines indicate the baseline flux during the flaring interval (Figure 1).

$T \sim 84 - 155$  days, and appears to be broadly divided into three  $\sim 8 - 10$  day long flare/delay sequences (Section 3.2), this could induce other smaller enhancements in the ACF over the studied interval.

As a cross-check of the lag derived from the full flaring interval  $\gamma$ -ray data, discrete ACFs were computed for two segments from  $T = 0 - 110$  and  $T = 110 - 265$  days. The lags obtained from Gaussian fits to the peaks were,  $\Delta t_\gamma = 11.52 \pm 0.31$  and  $\Delta t_\gamma = 11.38 \pm 0.28$  days, respectively, confirming the delay value and small uncertainty for the full interval, thus indicating that we obtained a robust measurement with the LAT. The small uncertainty in  $\Delta t_\gamma$  is competitive with the best determined radio measurements for B0218+357 although the former is marginally larger by  $\Delta t_\gamma - \Delta t_r = 1.0 \pm 0.3$  and  $1.4 \pm 0.8$  days ( $1\sigma$ ) than the Biggs et al. (1999) and

Cohen et al. (2000) values, respectively, but consistent with the Eulaers & Magain (2011) values. If the radio/ $\gamma$ -ray delays are intrinsically different due to an offset between the respective emitting regions, the implied offset in a singular isothermal sphere lens model is  $\sim 70$  pc (projected) for a  $\sim 10\%$  difference in the time delay. This seems extreme considering such offsets are on average  $\sim 7$  pc in other blazar jets (e.g., Pushkarev et al. 2010), and may rather suggest the uncertainty in the radio delay was underestimated (Section 1).

### 3.2. Flare Timescales

Utilizing the  $\gamma$ -ray delay measurement, we can broadly identify three sets of flare/delay episodes in the 6-hr binned LAT lightcurve of B0218+357 (Figure 2). The pre-flare times were what triggered the initial excitement



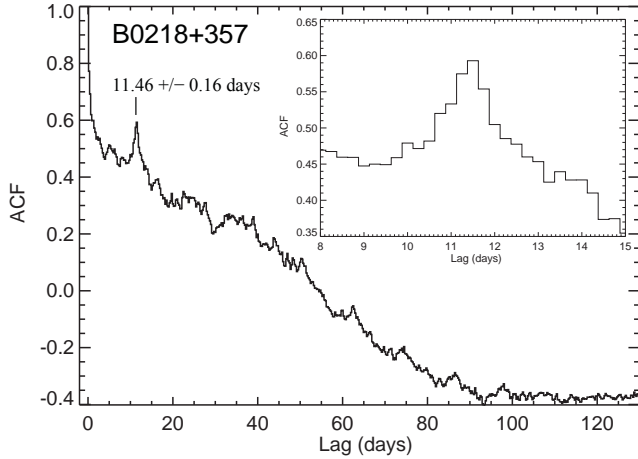


FIG. 3.— Auto-correlation function computed for the 6-hr binned LAT lightcurve of the 265-day flaring interval. The inset zooms in around the best-fit indicated lag peak.

in late 2012 August and are now detailed as a 6-hr flare at  $T \sim 50$  days (with a corresponding delayed signal 11.5 days later) and a doublet of 6 – 12-hr flares 1 day apart beginning at  $T \sim 65$  day. In the doublet, only the first flare showed a clear delayed flare 11.5 days later while the second shows no similar corresponding delayed (or 11.5-day prior) feature; microlensing (see below) or a relatively large variation in the magnification ratio are possible explanations.

The first bright  $\gamma$ -ray sequence began at  $T = 84$  day with the best-defined flaring structure with observed fluxes,  $\sim (2 - 5) \times 10^{-6}$  photons  $\text{cm}^{-2} \text{s}^{-1}$  over eight consecutive 6-hr bins, followed by a sharp drop and subsequent rise in one day. The *Fermi* ToO observation began 10 days later and the anticipated delayed emission mirrored the initial flare with the rise and peak separated by 1 day and all features well-matched 11.5 days later. We broadly identified two subsequent (2nd and 3rd)  $\sim 8 - 10$  day duration  $\gamma$ -ray flaring sequences, but these were more difficult to disentangle because of superposing flares in the integrated lightcurves. The post-flare intervals showed lower fluxes, comparable to the pre-flare emission states.

In Figure 2, the observed variability timescales (doubling and halving),  $t_{\text{var}}$ , during the first and subsequent two flaring episodes are securely less than the 6-hr binning. Doubling timescales as short as 2-orbits ( $\sim 3$  hrs) are further suggested in the orbit-by-orbit binned lightcurve from the *Fermi* ToO pointing of the first delayed flare (Figure 1, bottom). Such timescales are amongst the fastest well-constrained  $\gamma$ -ray variability in a blazar observed with the LAT (Tavecchio et al. 2010; Abdo et al. 2011) and constrain the  $\gamma$ -ray emission region diameter,  $d \leq 2ct_{\text{var}}/(1+z) \leq 6 \times 10^{14}$  cm, modulo the unknown Doppler beaming factor. Assuming an  $h = H_0/(100 \text{ km s}^{-1} \text{ Mpc}^{-1}) = 0.71$  ( $\Omega_M = 0.27$ ,  $\Omega_\Lambda = 0.73$ ) cosmology, this translates to an angular diameter  $\approx 30$  nano-arcseconds,  $\sim 10^4 \times$  smaller than the best radio size constraint (Mittal et al. 2007). Microlensing is thus an important factor in interpreting our  $\gamma$ -ray results because the smaller the structures, the larger the expected variability of magnification.

### 3.3. Flux and Magnification Ratios

Adopting the  $\gamma$ -ray delay, we compared the 6-hr binned lightcurves for the three main flaring episodes with the observations shifted by  $-11.46$  days and computed the observed ratios between corresponding flux pairs, retaining only ratio values  $\geq 2 \times$  their uncertainties (Figure 4). The first sequence appears to show the clearest correspondence between features in the two lightcurves, with only minor deviations about the weighted average flux ratio  $1.3 \pm 0.1$ . By subtracting a baseline,  $F_\gamma = 0.3 \times 10^{-6}$  photons  $\text{cm}^{-2} \text{s}^{-1}$  (the minimum observed flux during the overall flaring interval), we can further estimate a corresponding magnification ratio in  $\gamma$ -rays  $\approx 1.3$ , consistent with the flux ratio. The average ratios for this first sequence seem to imply the brighter A image led the B image in  $\gamma$ -rays, as observed in the radio. More conservatively however, given the large uncertainties in the individual measurements, the flux ratios appear consistent with unity. Moreover, for the subsequent 2nd and 3rd sequences, the correspondences between the flare and delayed emissions were less clear. Sharp and more scattered changes in the paired flux ratios were apparent, including values  $< 1$  (which would imply a fainter leading A image). We interpret this as an artifact due to contamination from superposing flares after the source has already entered a very active phase. This confusion in the integrated lightcurves prevents us from reliably determining magnification ratios, and how variable this quantity may have been.

The flux ratio measured in  $\gamma$ -rays is smaller than in the radio. Biggs et al. (1999) found a small, but statistically significant frequency dependence in the flux ratios,  $3.57 \pm 0.01$  (8 GHz) and  $3.73 \pm 0.01$  (15 GHz), while Cohen et al. (2000) found similar values but with larger uncertainty,  $3.2^{+0.3}_{-0.4}$  (8 GHz) and  $4.3^{+0.5}_{-0.8}$  (15 GHz). Frequency dependence in the flux ratios of the two radio images and their observed substructures could be possibly due to free-free absorption and scattering from a molecular cloud in the lens galaxy (Mittal et al. 2007). We note that the radio and  $\gamma$ -ray observations are not simultaneous and magnification ratios could be variable with time. Further complicating such comparisons are open questions in blazar jet studies, i.e., the radio and  $\gamma$ -ray emitting regions need not coincide, with the latter likely more compact (Section 3.2), and whether successive  $\gamma$ -ray flares originated in a single emission zone or from separate relativistically moving dissipation regions along the jet. Excursions could also be due to intrinsic changes in the magnification ratios or microlensing from the relative motion of the source seen through a clumpy lensing galaxy. Indeed, microlensing in the context of extremely compact  $\gamma$ -ray emission zones (Torres et al. 2003) could explain the single 6-hr flare points that do not have corresponding lags (marked with asterisks in Figure 2), although fast superposed flares are also a possibility. Note that in optical and infrared observations, the B image appears brighter than the A image, i.e., reversed from the radio situation, and this is likely due to a combination of extinction of the A image and microlensing (Falco et al. 1999; Jackson et al. 2000).

### 4. DISCUSSION AND CONCLUSIONS

Our detection of a gravitational lens time delay,  $\Delta t_\gamma = 11.46 \pm 0.16$  days, in the LAT observations of blazar B0218+357 has some interesting potential implications

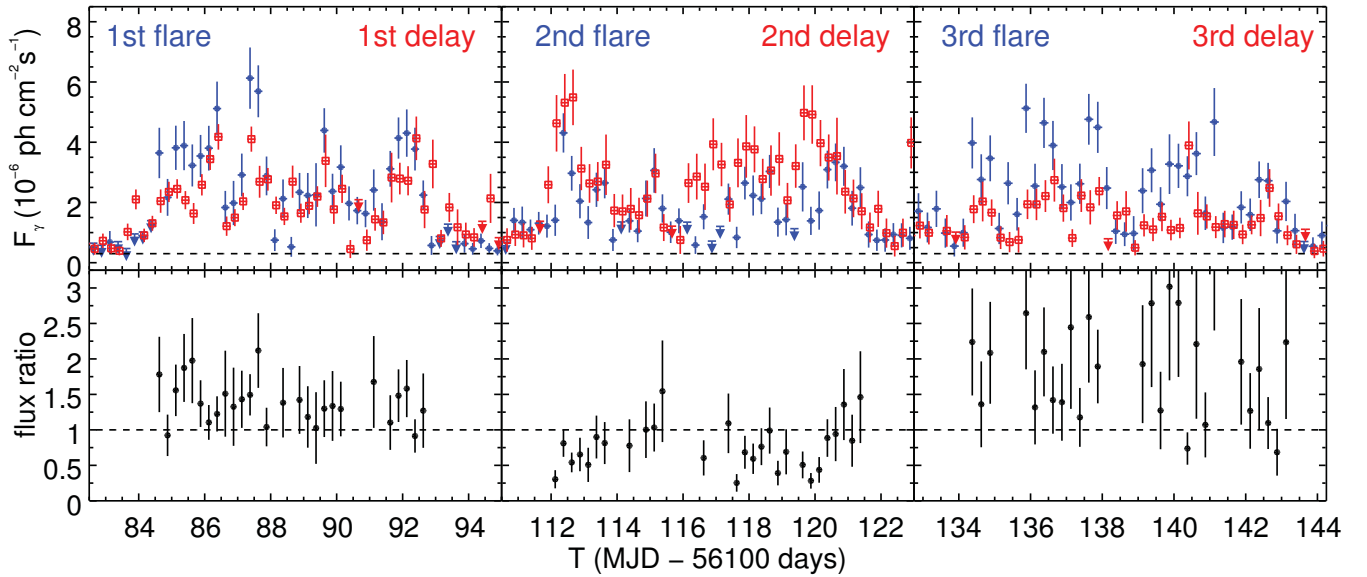


FIG. 4.— Top panels show the 6-hr binned lightcurves (Figure 2) for the three flares (filled blue) and delayed emission shifted by  $-11.46$  days (open red). Bottom panels show individual observed flux ratios (dashed line drawn at ratio = 1 for reference) in the corresponding upper panels; error bars are symmetric and the third panel was cropped in order to display a common range.

for future  $\gamma$ -ray studies. Foremost, the LAT detection of a  $\gamma$ -ray gravitational lens flaring event in B0218+357 suggests that such a measurement is possible in other blazars. In particular, gravitational lenses found in surveys of flat-spectrum radio sources (Browne et al. 2003; Winn et al. 2000) comprise a relevant sample as these form the basis of candidate  $\gamma$ -ray blazar catalogs (e.g., Healey et al. 2007). There are  $\sim 20$  gravitational lenses from these surveys out of  $> 10^4$  radio sources studied with  $\gtrsim 30$  mJy at 8 GHz and so far, the two radio brightest are detected  $\gamma$ -ray sources, PKS1830–211 (below) and B0218+357 (out of  $\sim 10^3$  known  $\gamma$ -ray blazars; Nolan et al. 2012). The other fainter lensed systems are typically less variable at radio frequencies, making delay measurements difficult (e.g., Jackson 2007; Eulaers & Magain 2011) and while they are not yet reported  $\gamma$ -ray sources, the all-sky monitoring of *Fermi*-LAT will allow the detection of short-timescale flaring  $\gamma$ -ray activity in which to attempt delay measurements. Importantly,  $\gamma$ -ray measurements constrain lens parameters free of propagation effects like scintillation (Heeschen 1984; Lovell et al. 2008) that can hamper radio delay attempts (Winn et al. 2004), although microlensing may be an important limiting factor because  $\gamma$ -ray emitting regions are expected to be more compact than in the radio.

The case of B0218+357 appears to be the first clear case of a  $\gamma$ -ray detected gravitational lens time delay for any astrophysical system. Previously,  $\gamma$ -ray flaring from the gravitationally lensed  $z = 2.507$  blazar PKS1830–211 was detected with the *Fermi*-LAT (Ciprini 2010) with a claimed delay,  $\Delta t_\gamma = 27.1 \pm 0.6$  days (Barnacka et al. 2011) consistent with the radio measurement,  $\Delta t_r = 26^{+4}_{-5}$  days (Lovell et al. 1998). Subsequent analysis of more LAT data, including several prominent flares, did not confirm the  $\gamma$ -ray delay (Abdo et al. 2013). If the  $\gamma$ -ray delay in PKS1830–211 is assumed to be the same as

the radio-measured delay, the non-detection of delayed  $\gamma$ -ray flares implies a magnification ratio in  $\gamma$ -rays much larger ( $\gtrsim 6$ ) than that observed in the radio ( $1.52 \pm 0.05$ ; Lovell et al. 1998), thus opposite of what we observed in B0218+357. With only two examples studied, no trend is clear. However, if microlensing effects can be disentangled (and in fact utilized as additional constraints on the emitting region source size), magnification ratios in radio and  $\gamma$ -ray arising from spatially distinct emission regions may be utilized as a probe of differing multi-frequency jet structures (see Martí-Vidal et al. 2013).

A time delay due to gravitational lensing of a background source by a foreground object can constrain Hubble’s parameter (Refsdal 1964). The original lens model for B0218+357 (Biggs et al. 1999) predicted a delay,  $\Delta t = 7.2^{+1.3}_{-2.0} h^{-1}$  days (95% confidence). Utilizing improved localization of the lensing galaxy, the delay model uncertainty was reduced to 6.0% (York et al. 2005), thus deriving  $h = 0.70 \pm 0.05$ , assuming the often quoted Biggs et al. (1999) measured radio delay (cf., Section 3.1). Adopting the York model for our independent  $\gamma$ -ray measured delay results in  $h = 0.64 \pm 0.04$ , where this quoted uncertainty is due only to the time delay estimate and the statistical uncertainty in the mass model. Systematic errors in the modeling, and additional uncertainty due to line-of-sight structures (e.g., Suyu et al. 2012) will likely significantly increase this. Nevertheless, it is interesting that the LAT time delay brings the estimated value of Hubble’s constant down, towards the low end of modern measurements (e.g., Planck Collaboration 2013). An underdense environment would require this inferred  $h$  value to increase; including external lensing effects in future cosmographic analyses might be important in this system. Moreover, since the radio and  $\gamma$ -ray emission regions are likely not co-spatial, the assumed radio-derived time-delay function values may be inaccurate. A fully self-consistent joint modeling of the radio

and  $\gamma$ -ray source is needed to resolve this. If the LAT can measure a lag in the  $\gamma$ -ray lightcurve of one of the previously known systems with wider separation or in a new example (below), this can give independent  $\gamma$ -ray based constraints on Hubble's constant.

One exciting result would be the detection of a lens delay in a flaring  $\gamma$ -ray source that is not yet identified as a gravitationally lensed system at radio wavelengths or otherwise. These could possibly be lensed image pairs with flat-spectrum radio sources at smaller separations than in the  $0.2''$  resolution of VLA surveys (references above). Similar radio lens surveys in the southern hemisphere are not yet as complete (e.g., Prouton et al. 1999), so a  $\gamma$ -ray delay signature in their LAT lightcurves could betray the presence of a previously unknown lens system. Such a strategy has been proposed for future wide-field optical surveys (Pindor 2005), and the discovery potential of the LAT in  $\gamma$ -rays should now be recognized. Furthermore, with the different flux ratios at radio and  $\gamma$ -ray wavelengths, and possible variability of

the ratio, some sources could be bright in  $\gamma$ -rays and less conspicuous at radio. Such potential gravitational lenses could be hidden in plain sight within the radio catalogs used for blazar associations in LAT catalogs, or could be amongst the currently unidentified  $\gamma$ -ray sources (Torres et al. 2002).

The *Fermi*-LAT Collaboration acknowledges support from a number of agencies and institutes for both development and the operation of the LAT as well as scientific data analysis. These include NASA and DOE in the United States, CEA/Irfu and IN2P3/CNRS in France, ASI and INFN in Italy, MEXT, KEK, and JAXA in Japan, and the K.A. Wallenberg Foundation, the Swedish Research Council and the National Space Board in Sweden. Additional support from INAF in Italy and CNES in France for science analysis during the operations phase is also gratefully acknowledged. C.C.C. was supported at NRL in part by NASA DPR S-15633-Y.

*Facilities:* Fermi

## REFERENCES

- Abdo, A. A., Ackermann, M., Ajello, M., et al. (*Fermi*-LAT Collaboration) 2010, *ApJ*, 722, 520
- . 2011, *ApJ*, 733, L26
- . 2013, submitted (lensed blazar PKS1830–211)
- Ackermann, M., Ajello, M., Albert, A., et al. (*Fermi*-LAT Collaboration) 2012, *ApJS*, 203, 4
- Atwood, W. B., 2007, in the Les Houches Winter School “The Violent Universe,” March 2007, CEA-Saclay
- Atwood, W. B., Abdo, A. A., Ackermann, M., et al. (*Fermi*-LAT Collaboration) 2009, *ApJ*, 697, 1071
- Barnacka, A., Glicenstein, J.-F., & Moudden, Y. 2011, *A&A*, 528, L3
- Biggs, A. D., Browne, I. W. A., Helbig, P., et al. 1999, *MNRAS*, 304, 349
- Browne, I. W. A., Patnaik, A. R., Walsh, D., & Wilkinson, P. N. 1993, *MNRAS*, 263, L32
- Browne, I. W. A., Wilkinson, P. N., Jackson, N. J. F., et al. 2003, *MNRAS*, 341, 13
- Cheung, C. C., Ojha, R., Orienti, M., Wood, D. L. (*Fermi*-LAT Collaboration) 2012, *The Astronomer's Telegram*, 4411, 1
- Ciprini, S. (*Fermi*-LAT Collaboration) 2010, *The Astronomer's Telegram*, 2943, 1
- . 2012, *The Astronomer's Telegram*, 4343, 1
- Cohen, A. S., Hewitt, J. N., Moore, C. B., & Haarsma, D. B. 2000, *ApJ*, 545, 578
- Cohen, J. G., Lawrence, C. R., & Blandford, R. D. 2003, *ApJ*, 583, 67
- Corbet, R., Cheung, C. C., Kerr, M., & Ray, P. S. 2012, 4th International Fermi Symposium Proceedings, eConf C121028, 21, arXiv:1302.5141
- Corbett, E. A., Browne, I. W. A., Wilkinson, P. N., & Patnaik, A. 1996, in *Astrophysical Applications of Gravitational Lensing*, Eds. C. S. Kochanek & J. N. Hewitt, IAU Symp. 173, 37
- Edelson, R. A., & Krolik, J. H. 1988, *ApJ*, 333, 646
- Eulaers, E., & Magain, P. 2011, *A&A*, 536, A44
- Falco, E. E., Impey, C. D., Kochanek, C. S., et al. 1999, *ApJ*, 523, 617
- Ghisellini, G., Tavecchio, F., Foschini, L., et al. 2010, *MNRAS*, 402, 497
- Giroletti, M., Orienti, M., & Cheung, C. C. (*Fermi*-LAT Collaboration) 2012, *The Astronomer's Telegram*, 4371, 1
- Healey, S. E., Romani, R. W., Taylor, G. B., et al. 2007, *ApJS*, 171, 61
- Heeschen, D. S. 1984, *AJ*, 89, 1111
- Jackson, N. 2007, *Living Reviews in Relativity*, 10, 4
- Jackson, N., Xanthopoulos, E., & Browne, I. W. A. 2000, *MNRAS*, 311, 389
- Lovell, J. E. J., Jauncey, D. L., Reynolds, J. E., et al. 1998, *ApJ*, 508, L51
- Lovell, J. E. J., Rickett, B. J., Macquart, J.-P., et al. 2008, *ApJ*, 689, 108
- Martí-Vidal, I., Muller, S., Combes, F., et al. 2013, *A&A*, 558, A123
- Mattox, J. R., Bertsch, D. L., Chiang, J., et al. 1996, *ApJ*, 461, 396
- Mittal, R., Porcas, R., & Wucknitz, O. 2007, *A&A*, 465, 405
- Nolan, P. L., Abdo, A. A., Ackermann, M., et al. (*Fermi*-LAT Collaboration) 2012, *ApJS*, 199, 31
- O’Dea, C. P., Baum, S. A., Stanghellini, C., et al. 1992, *AJ*, 104, 1320
- Patnaik, A. R., Browne, I. W. A., Wilkinson, P. N., & Wrobel, J. M. 1992, *MNRAS*, 254, 655
- Patnaik, A. R., Browne, I. W. A., King, L. J., et al. 1993, *MNRAS*, 261, 435
- Pauliny-Toth, I. I. K., & Kellermann, K. I. 1972, *AJ*, 77, 797
- Peterson, B. M., Wanders, I., Horne, K., et al. 1998, *PASP*, 110, 660
- Pindor, B. 2005, *ApJ*, 626, 649
- Planck Collaboration, Ade, P. A. R., Aghanim, N., et al. 2013, arXiv:1303.5076
- Prouton, O. R., Warren, S. J., & Wright, A. E. 1999, in *Gravitational Lensing: Recent Progress and Future Goals*, Eds. T.G. Brainerd & C.S. Kochanek, arXiv:astro-ph/9909304
- Pushkarev, A. B., Kovalev, Y. Y., & Lister, M. L. 2010, *ApJ*, 722, L7
- Refsdal, S. 1964, *MNRAS*, 128, 307
- Suyu, S. H., Hensel, S. W., McKean, J. P., et al. 2012, *ApJ*, 750, 10
- Tavecchio, F., Ghisellini, G., Bonnoli, G., & Ghirlanda, G. 2010, *MNRAS*, 405, L94
- Torres, D. F., Romero, G. E., & Eiroa, E. F. 2002, *ApJ*, 569, 600
- Torres, D. F., Romero, G. E., Eiroa, E. F., Wambsganss, J., & Pessah, M. E. 2003, *MNRAS*, 339, 335
- Winn, J. N., Hewitt, J. N., Schechter, P. L., et al. 2000, *AJ*, 120, 2868
- Winn, J. N., Lovell, J. E. J., Bignall, H., et al. 2004, *AJ*, 128, 2696
- Wucknitz, O., Biggs, A. D., & Browne, I. W. A. 2004, *MNRAS*, 349, 14
- York, T., Jackson, N., Browne, I. W. A., Wucknitz, O., & Skelton, J. E. 2005, *MNRAS*, 357, 124